Ishikawa and Matsumoto *Earth, Planets and Space* 2014, **66**:35
http://www.earth-planets-space.com/content/66/1/35

Earth, Planets and Space
a SpringerOpen Journal

LETTER **Open Access**

Effect of fluid H_2O on compressional wave velocities in quartz aggregate up to 500°C at 0.5 GPa

Masahiro Ishikawa* and Yuki Matsumoto

Abstract

Compressional wave velocities (*V*p) in quartz aggregate were measured to quantify the effect of pore fluid (H_2O) on *V*p at high pressure-temperature (*P-T*). Ultrasonic measurements were conducted on dry and wet quartz aggregate from room temperature to 500°C at 0.5 GPa using a piston cylinder apparatus. The experiment showed a 4% decrease in measured *V*p in quartz aggregate with increasing H_2O content to 1 wt.%, whereas the temperature derivative of *V*p ($\partial Vp/\partial T = -2.8$ to -4.9×10^{-4} km s^{-1}°C^{-1}) in wet quartz aggregate remained almost the same as for the dry quartz aggregate ($\partial Vp/\partial T = -5.2 \times 10^{-4}$ km s^{-1}°C^{-1}). Our high-pressure, high-temperature experiments show that a small amount of pore fluid (0.4 to 1.0 wt.% H_2O) can significantly reduce *V*p under the *P-T* conditions of the middle crust.

Keywords: *V*p; Fluid; Quartz

Findings

Background

Seismic tomography studies show lateral changes in velocities within the crust. The first observation of a low seismic velocity (−5%) and high Poisson's ratio (+6%) anomaly at the hypocentral zone of the 1995 Kobe earthquake (magnitude 7.2) in Japan demonstrated that pore fluids (such as fluid H_2O) could be critical to earthquake studies (Zhao et al. 1996; Zhao and Mizuno 1999). Therefore, seismic velocities have become vital parameters in our understanding of the dynamics of the Earth's crust. To estimate the pore fluid content in the crust, it is important to investigate the effect of pore fluids on the elastic velocities of crustal materials under realistic pressure-temperature (*P-T*) conditions of the deep crust. In this paper, we measured elastic wave velocities in dry and wet quartz aggregates at pressures up to 0.5 GPa and temperatures up to 500°C, which correspond to those of the Earth's middle crust.

The first ultrasonic velocity measurement system was developed by McSkimin (1950), and it has been further developed and adapted to high-pressure techniques (e.g., Li et al. 1998). The elastic velocities in many crustal rock types have been determined by ultrasonic experiments using high-pressure apparatus (e.g., Christensen and Mooney 1995; Ito and Tatsumi 1995; Mueller 1995; Rudnick and Fountain 1995; Kern et al. 1997). These experimental studies have provided compressional and shear wave velocity data that can be used to constrain the petrological characteristics of the lower continental crust. However, the effect of pore fluids such as water on the elastic wave velocities of crustal rocks at high temperatures and under deep crustal pressure is still far from understood.

In this paper, we investigate the effect of fluid H_2O on compressional velocities (*V*p) in quartz aggregate. Our results demonstrate that the compressional wave velocity decreases significantly at 1 wt.% H_2O (present as pore fluid) under the *P-T* conditions of the middle crust.

Methods

The high-pressure apparatus and layout of the experimental system for conducting the ultrasonic experiments in this study are shown in Figure 1. The elements of this experimental setup included a piston cylinder press and an ultrasonic system. We used a solid-medium piston cylinder apparatus with an internal diameter of 34 mm and a length of 80 mm (Toshiba Tungaloy Company, Kawasaki

---

* Correspondence: ishikawa@ynu.ac.jp
Graduate School of Environment and Information Sciences, Yokohama National University, 79-7 Tokiwadai, Hodogaya-ku, Yokohama 2408501, Japan

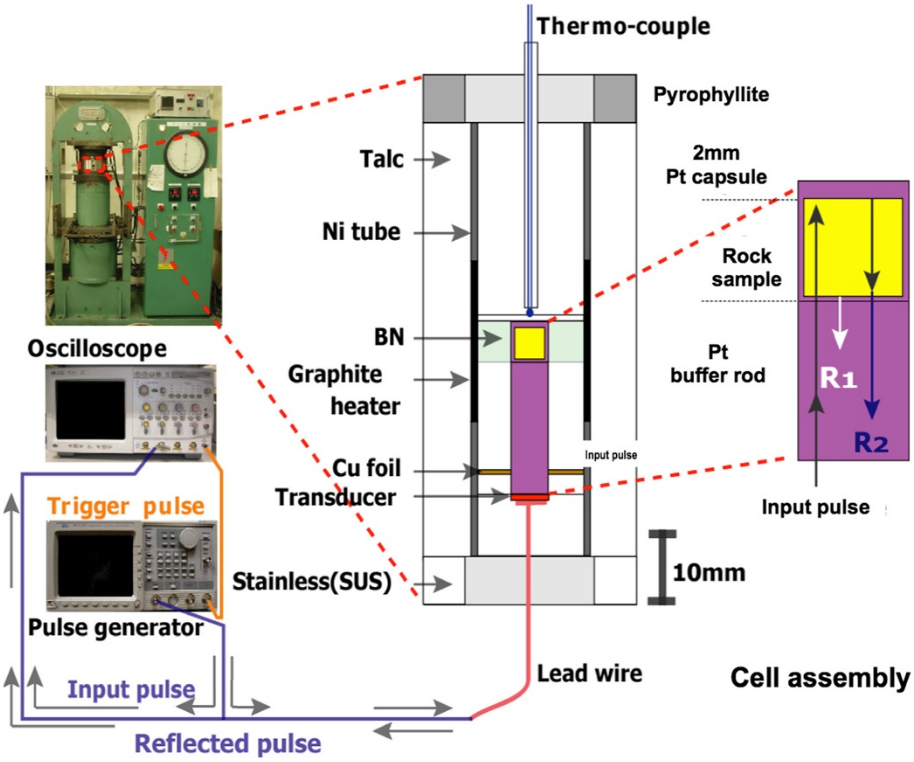

Figure 1 Layout of ultrasonic experimental system using pulse reflection technique and schematic diagram of high-pressure cell.

City, Japan). Talc, pyrophyllite, and boron nitride (BN) were used as the solid pressure transmitting medium that also contained a heating element and sample. The calibration of pressure has been described elsewhere (Kono et al. 2004, 2008; Kozai and Arima 2005; Nishimoto et al. 2005).

Both top and bottom faces of the core sample (approximately 6.0 mm diameter and 6.0 mm length) were diamond-polished. Each core sample was vacuum-dried at 180°C for 24 h. The vacuum-dried samples were then encapsulated in platinum with or without distilled water. A 20-mm long platinum buffer rod was placed between the platinum-encapsulated sample and a $LiNbO_3$ piezoelectric transducer. The piezoelectric transducer was mounted on the bottom of the platinum buffer rod. No glue was used at any interface. The encapsulated sample, buffer rod, and piezoelectric transducer were then placed in the talc pyrophyllite high-pressure cell. High temperatures were achieved using a graphite heater and were monitored by a Pt-$PtRh_{13}$ thermocouple. A thermocouple junction was placed on the top of the platinum-encapsulated sample. The temperature differences between the thermocouple junction and several parts of the cylindrical rock sample were measured to evaluate the thermal distribution of the cell assembly (Kono et al. 2004, 2008). Figure 1 also shows details of the high-pressure, high-temperature cell assembly inside the cylinder.

Ultrasonic velocity measurements were performed using the pulse reflection technique with buffer rod. To generate elastic waves, sinusoidal electric burst signals were produced by an arbitrary waveform generator (Tektronix AWG2021, Beaverton, OR, USA) and applied to the $LiNbO_3$ piezoelectric transducer (10° Y-cut). The elastic waves of 8 MHz were transmitted through the buffer rod and the sample. The sample length was more than ten times longer than the wavelength of the elastic waves. Reflected elastic waves from the top and bottom surfaces of the sample were received by the transducer and then converted into an electric signal. The waveforms were recorded using a digital oscilloscope (Hewlett-Packard 54825A, Palo Alto, CA, USA). These signals were sampled 4,096 times for each run at a sample rate of 1.0×10^9 samples/s for a given *P-T* condition. We used the mean value of the recorded travel time for a given *P-T* condition and corresponding ray path to compute the average velocity. The maximum uncertainty in the measured *V*p values was ±0.4%. This procedure is described in more detail elsewhere (Kono et al. 2004).

The rock sample used in this study was a natural quartz aggregate (fine-grained silicified rock with a density of 2.58 g/cm^3 and porosity of 3.2 vol.%) that was collected from the Iwakuni-Yanai area in the Ryoke belt, SW Japan (Yamamoto et al. 2004; Matsumoto et al. 2010). The

Ryoke belt in this area is mainly composed of a metamorphosed Jurassic accretionary complex and Cretaceous granites (Ikeda 1998). Fine-grained silicified rocks occur in pelitic schist of the biotite zone and in the northernmost part of the cordierite zone (Yamamoto et al. 2004). The sample used in this study was composed mainly of quartz (about 90 vol.%) with minor muscovite, biotite, feldspar, and opaque minerals (Figure 2), which were <50 μm in grain size. The rock shows a granoblastic and nearly isotropic texture.

Results and discussion

The measurements were carried out up to 0.5 GPa (wet samples) or 0.6 GPa (dry samples) at temperatures ranging up to 500°C using a piston cylinder apparatus and the techniques described above. In this experiment, the pressure was first increased to 0.5 GPa (wet samples) or 0.6 GPa (dry samples) at room temperature and then the temperature was increased to 500°C. To ensure a steady state travel time, we kept the *P-T* conditions of the experiment constant for 30 to 180 min before performing the velocity measurements. The sample recovered elastically and retained its original length, which suggests that it had not been subjected to plastic deformation during the entire experiment. The compressional wave velocities are plotted against pressure in Figure 3 and against temperature in Figure 4.

As shown in Figure 3, the compressional velocities in the dry sample increased rapidly until a pressure of approximately 0.3 GPa was reached. The increase in *V*p was probably attributable to the closure of microcracks (e.g., Birch 1960; Kern 1982). The compressional wave velocities also showed a linear increase at higher pressure between 0.3 and 0.6 GPa, which suggests that the effect of porosity on the measured velocities was not significant within this pressure range. By fitting velocity data using linear functions of pressure, we obtained the pressure derivative $\partial V\mathrm{p}/\partial P = 0.29$ km s^{-1} GPa^{-1}. The pressure derivative (in the range $P = 0.3$ to 0.6 GPa) was then used to linearly extrapolate the velocity data, which yielded a *V*p value of 6.04 km s^{-1} under ambient conditions. This is the so-called intrinsic velocity of Kern (2011). As in previous studies (Shingai et al. 2001; Kitamura et al. 2003; Kono et al. 2004; Nishimoto et al. 2005; Ishikawa et al. 2008), linear trends of velocity as a function of pressure were observed above a threshold pressure of between 0.3 and 0.6 GPa. At lower pressures, the velocities of the samples are compromised by unclosed pore spaces filled with air.

The dry sample was heated from room temperature at 0.5 GPa to 500°C. Unfortunately, the lead wire was disconnected from the piezoelectric transducer within the high-pressure cell at 500°C and therefore *V*p could not be measured at 500°C. As the temperature increased to 400°C, the compressional velocities decreased from 6.19 to 5.99 km s^{-1} (Figure 4). By fitting the velocity data using linear functions of temperature, we obtained the temperature derivative $\partial V\mathrm{p}/\partial T = -0.52 \times 10^{-3}$ km s^{-1}°C^{-1}. Because the compressibility and thermal expansion of low quartz is less than 0.5% between ambient conditions and 0.5 GPa and 400°C (e.g., Raz et al. 2002), the changes of sample length can be considered to be insignificant for the determination of *V*p.

To understand the effect of water on *V*p, we measured the compressional wave velocities in wet samples (Figures 3 and 4). In each experiment involving a wet sample, the pressure was first increased to 0.5 GPa at room temperature (Figure 3). The compressional velocities increased rapidly up to a pressure of 0.3 GPa. This is probably attributable to the closure of air-filled pore spaces. The compressional wave velocities also increased linearly at higher pressures between 0.3 and 0.5 GPa, and these values showed a similar pressure dependence for different H_2O contents, which suggests that the effect of pore air on the measured velocities is not significant within this pressure range. By fitting velocity data using linear functions of pressure, we obtained the pressure derivative $\partial V\mathrm{p}/\partial P = 0.45$ km s^{-1} GPa^{-1} for 0.37 wt.% H_2O and 0.54 km s^{-1} GPa^{-1} for 0.98 wt.% H_2O. As before, we used the pressure derivative to linearly extrapolate the velocity data (in the range $P = 0.3$ to 0.5 GPa) to ambient conditions, which resulted in an intrinsic *V*p of 5.79 km s^{-1} for 0.37 wt.% H_2O and 5.65 km s^{-1} for 0.98 wt.% H_2O. After pressurization to 0.5 GPa, the sample was heated to 500°C (Figure 4), which caused the compressional velocities of the quartz aggregate with 0.37 wt.% H_2O to decrease from 6.02 to 5.79 km s^{-1}. By fitting the velocity data using linear functions of temperature, we obtained the temperature derivative $\partial V\mathrm{p}/\partial T = -0.49 \times 10^{-3}$ km s^{-1}°C^{-1} for quartz aggregate with 0.37 wt.% H_2O. After repeating the

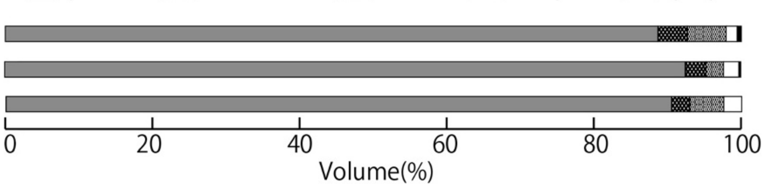

Figure 2 Modal compositions of the quartz aggregate samples used in this study. Top, dry; middle, 0.37 wt.% H_2O; bottom, 0.98 wt.% H_2O.

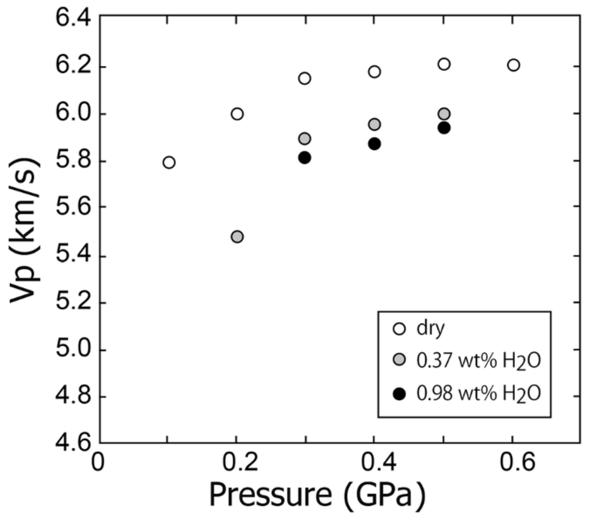

Figure 3 **Plot of the measured *V*p of quartz aggregate versus pressure at 25°C.**

experiment using quartz aggregate with 0.98 wt.% H_2O, the compressional velocity decreased from 5.92 to 5.78 km/s as the temperature increased to 500°C. By fitting the velocity data using linear functions of temperature, we obtained $\partial Vp/\partial T = -0.28 \times 10^{-3}$ km s^{-1}°C^{-1}. Comparison of the temperature derivatives of wet samples with that of the dry sample showed that the temperature derivatives were insensitive to the addition of fluid H_2O within the 1 wt.% range investigated.

The velocity drop is plotted against temperature in Figure 5. We used the following definition of the velocity drop:

$$\text{Velocity drop} = 100 \times \left[V\mathrm{p}_{(\mathrm{dry},\quad P=0.5\,\mathrm{GPa},T)} - V\mathrm{p}_{(\mathrm{wet},\quad P=0.5\,\mathrm{GPa},T)}\right] / V\mathrm{p}_{(\mathrm{dry},\quad P=0.5\,\mathrm{GPa},\mathrm{T})}$$

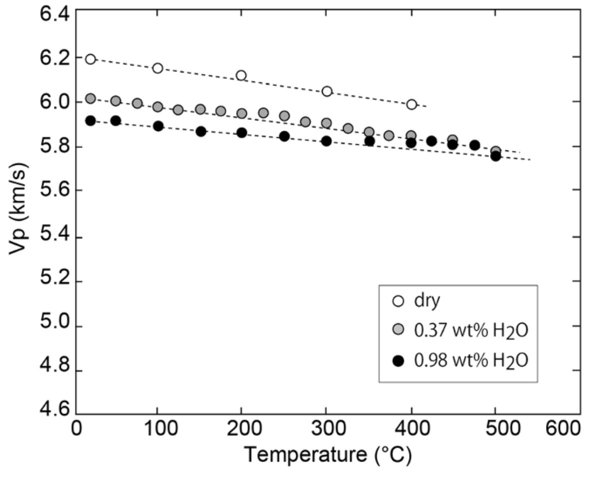

Figure 4 **Plot of the measured *V*p of quartz aggregate against temperature at 0.5 GPa.**

The velocity drop was approximately 3% in the experiment using quartz aggregate with 0.37 wt.% H_2O. In the experiment with higher H_2O content (0.98 wt.% H_2O), the velocity drop remained constant (4%) up to 200°C and then decreased slightly to 3% with increasing temperature.

Zhao et al. (1996) reported a low seismic velocity (−5%) and high Poisson's ratio (+6%) anomaly extending over approximately 300 km^2 at the hypocentral zone of the magnitude 7.2 Kobe earthquake that occurred on January 17, 1995. They speculated that this anomaly was due to an over-pressurized, fluid-filled, fractured rock matrix that contributed to the initiation of the Kobe earthquake. The low velocity anomaly (−5%) is almost equivalent to the velocity drop (−4%) shown in our experimental results with 1 wt.% H_2O. Our results also show that the addition of 0.4 to 1.0 wt.% H_2O into the quartz aggregate causes a velocity drop of 3% to 4% at the pressures and temperatures of the middle crust (0.5 GPa, 25°C to 500°C), which suggests that one possible reason for low seismic velocities (−5%) is 1 wt.% H_2O fluid-filled rock in the hypocentral zone. At this stage, we see our experimental data as a useful contribution towards improved quantitative understanding of the effect of H_2O on the elastic wave velocities of rocks. We also hope our results will be useful for determining the geofluid distribution within the crust, thereby enhancing future interpretations of seismic tomographic data.

Summary

A compressional wave velocity of $Vp = 6.04$ km s^{-1} for dry quartz aggregate under ambient conditions was determined by linear backward extrapolation of the velocity data recorded at high pressures (0.4 to 0.6 GPa). The pressure derivatives obtained by fitting the high pressure data of 0.4 to 0.6 GPa yielded $\partial Vp/\partial P = 0.29$ km s^{-1} GPa^{-1}. The temperature derivatives obtained at

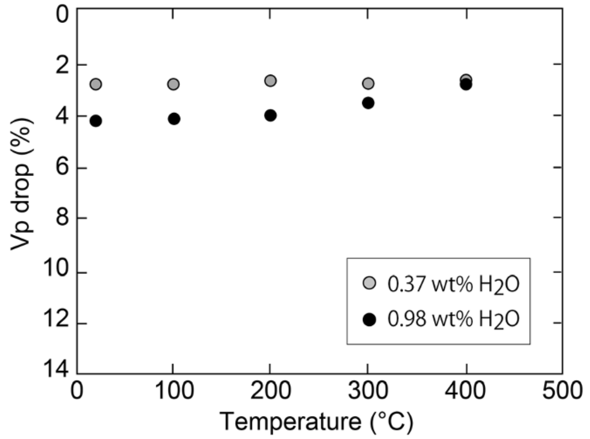

Figure 5 **Plot of velocity drop against temperature.**

a pressure of 0.5 GPa and temperatures from 25°C to 400°C yielded $\partial Vp/\partial T = -0.52 \times 10^{-3}$ km s^{-1} °C^{-1}.

The compressional wave velocities at ambient conditions were determined to be $Vp = 5.79$ km s^{-1} for wet quartz aggregate of 0.37 wt.% H_2O and $Vp = 5.65$ km s^{-1} for wet quartz aggregate of 0.98 wt.% H_2O. These values were determined using backward extrapolation from the velocity data at higher pressure (0.4 to 0.6 GPa). The pressure derivatives obtained by fitting the high pressure data of 0.4 to 0.6 GPa yielded $\partial Vp/\partial P = 0.45$ km s^{-1} GPa^{-1} for the 0.37 wt.% H_2O sample and 0.54 km s^{-1} GPa^{-1} for the 0.98 wt.% H_2O sample. The temperature derivatives obtained at a pressure of 0.5 GPa and temperatures from 25°C to 500°C yielded $\partial Vp/\partial T = -0.49 \times 10^{-3}$ km s^{-1}°C^{-1} for quartz aggregate with 0.37 wt.% H_2O and $\partial Vp/\partial T = -0.28 \times 10^{-3}$ km s^{-1}°C^{-1} for quartz aggregate with 0.98 wt.% H_2O.

Our results demonstrate that the magnitude of the velocity drop is dependent on the degree of saturation of the pore spaces with fluid H_2O. The velocity drop was approximately 3% with 0.37 wt.% H_2O and 3% to 4% with 0.98 wt.% H_2O. Hence, a small amount of pore fluid (0.4 to 1.0 wt.%), in this case, water, can significantly reduce the compressional wave velocity under the P–T conditions of the middle crust.

Competing interests

The authors declare that they have no competing interests.

Authors' contributions

MI and YM carried out the experimental works. YM carried out analytical works. MI organized the project and drafted the manuscript. All authors read and approved the final manuscript.

Acknowledgements

The authors would like to thank M. Arima and Y. Kono for their kind support in performing the high-pressure experiments. The authors are also grateful to M. Terabayashi for providing rock samples. This study was partly supported by Grants-in-Aid for Scientific Research provided by the Japanese Society for the Promotion of Science; these grants were provided to MI (23340153) and T. Matsuzawa (21109002).

Received: 15 December 2013 Accepted: 23 April 2014
Published: 15 May 2014

References

Birch F (1960) The velocity of compressional waves in rocks to 10 kbar: part 1. J Geophys Res 65:1083–1102

Christensen NI, Mooney WD (1995) Seismic velocity structure and composition of the continental crust: a global view. J Geophys Res 100:9761–9788

Ikeda T (1998) Progressive sequence of reactions of the Ryoke metamorphism in the Yanai district, southwest Japan: the formation of cordierite. J Metamorph Geol 16:39–52

Ishikawa M, Shingai E, Arima M (2008) Elastic properties of high-grade metamorphosed igneous rocks from Enderby Land and eastern Dronning Maud Land, Antarctica: evidence for biotite-bearing mafic lower crust. In: Satish-Kumar M et al (eds) Geodynamic Evolution of East Antarctica: A Key to the East–West Gondwana Connection, Geological Society, vol 308. Special Publications, London, pp 183–194. doi:10.1144/SP308.9

Ito K, Tatsumi Y (1995) Measurement of elastic wave velocities in granulite and amphibolite having identical H_2O-free bulk compositions up to 850°C at 1 GPa. Earth Planet Sci Lett 133:255–264

Kern H (1982) P- and S-wave velocities in crustal and mantle rocks under the simultaneous action of high confining pressure and high temperature and the effect of rock microstructure. In: Schreyer W (ed) High-Pressure Researches in Geosciences. E. Schweizerbart'sche Verlagsbuchhandlung, Stuttgart, pp 15–45

Kern H (2011) Measuring and modeling of P- and S-wave velocities on crustal rocks: a key for the interpretation of seismic reflection and refraction data. Int J Geophysics 530728:9, pages, http://dx.doi.org/10.1155/2011/530728

Kern H, Liu B, Popp T (1997) Relationship between anisotropy of P and S wave velocities and anisotropy of attenuation in serpentinite and amphibolite. J Geophys Res 102:3051–3065

Kitamura K, Ishikawa M, Arima M (2003) Petrological model of the northern Izu–Bonin–Mariana arc crust: constraints from high-pressure measurements of elastic wave velocities of the Tanzawa plutonic rocks, central Japan. Tectonophysics 371:213–221

Kono Y, Ishikawa M, Arima M (2004) Discontinuous change in temperature derivative of Vp in lower crustal rocks. Geophys Res Lett 31, L22601. doi:10.1029/2004GL020964

Kono Y, Miyake A, Ishikawa M, Arima M (2008) Temperature derivatives of elastic wave velocities in plagioclase ($An_{51\pm1}$) above and below the order–disorder transition temperature. Am Mineral 93:558–564

Kozai Y, Arima M (2005) Experimental study on diamond dissolution in kimberlitic and lamproitic melts at 1300–1420°C and 1 GPa with controlled oxygen partial pressure. Am Mineral 90:1759–1766

Li B, Chen G, Gwanmesia GD, Liebermann RC (1998) Sound velocity measurements at mantle transition zone conditions of pressure and temperature using ultrasonic interferometry in a multi-anvil apparatus. Manghnani MH, Yagi T (eds) Properties of Earth and Planetary Materials at High Pressure and Temperature, American Geophysical Union., pp 41–61

Matsumoto Y, Ishikawa M, Terabayashi M, Arima M (2010) Simultaneous measurements of compressional wave and shear wave velocities, Poisson's ratio, Vp/Vs under deep crustal pressure and temperature conditions: example of silicified pelitic schist from Ryoke belt, SW Japan. Island Arc 19:30–39

McSkimin HJ (1950) Ultrasonic measurement techniques applicable to small solid specimens. J Acoust Soc Am 22:413–418

Mueller HJ (1995) Modeling the lower crust by simulation of the in situ conditions: an example from the Saxonian Erzgebirge. Phys Earth Planet Inter 92:3–15

Nishimoto S, Ishikawa M, Arima M, Yoshida T (2005) Laboratory measurement of P-wave velocity in crustal and upper mantle xenoliths from Ichino-megata, NE Japan: ultrabasic hydrous lower crust beneath the NE Honshu arc. Tectonophysics 396:245–259

Raz U, Girsperger S, Thompson AB (2002) Thermal expansion, compressibility and volumetric changes of quartz obtained by single crystal dilatometry to 700°C and 3.5 kilobars (0.35 GPa). Eidgenössische Technische Hochschule Zürich, Department of Earth Sciences., http://dx.doi.org/10.3929/ethz-a-004392716

Rudnick RL, Fountain DM (1995) Nature and composition of the continental crust: a lower crustal perspective. Rev Geophysics 33:267–309

Shingai E, Ishikawa M, Arima M (2001) P-wave velocity in ultrahigh temperature granulites from the Archean Napier Complex, East Antarctica. Polar Geoscience 14:165–179

Yamamoto H, Terabayashi M, Oasa H, Kaneko Y, Anma R (2004) Competence contrast between pelitic schist and silicified pelitic schist in the Iwakuni-Yanai area of the Ryoke Belt, southwest Japan. J Geol Soc Jpn 110:119–122 (in Japanese with English abstract)

Zhao D, Mizuno T (1999) Crack density and saturation rate in the 1995 Kobe earthquake region. Geophys Res Lett 26:3213–3216

Zhao D, Kanamori H, Negishi H, Wiens D (1996) Tomography of the source area of the 1995 Kobe earthquake: evidence for fluids at the hypocenter? Science 274:1891–1894

doi:10.1186/1880-5981-66-35
Cite this article as: Ishikawa and Matsumoto: **Effect of fluid H_2O on compressional wave velocities in quartz aggregate up to 500°C at 0.5 GPa.** *Earth, Planets and Space* 2014 **66**:35.